Gravity and inertia effects in plate coating

Alain de Ryck, D Quere

Gravity and Inertia Effects in Plate Coating

Alain de Ryck* and David Quéré†,[1]

*École des Mines d'Albi-Carmaux, route de Teillet, 81013 Albi CT Cedex 09, France; and †Laboratoire de Physique de la Matière Condensée, URA 792 du CNRS, Collège de France, 75231 Paris Cedex 05, France

Coating processes are of technological interest. We focus here on the extraction of a vertical plate out of a wetting liquid. We first summarize the Landau-Levich-Derjaguin theory, including the gravity corrections which have been proposed in particular by White and Tallmadge. We propose a new numerical solution to the problem. Then, we discuss further developments: for liquids of low viscosity, it is shown that above a threshold in capillary number, the film is thickened because of inertia. A simple scaling argument is proposed for predicting the location of the threshold.

Key Words: **fluid coating; thin liquid films; wetting.**

1. INTRODUCTION

When a plate is drawn out of a wetting liquid bath (viscosity η, surface tension γ, and specific mass ρ) at a velocity V, it comes out coated with a liquid film whose thickness e was first derived by Landau, Levich, and Derjaguin (1, 2). At low velocities, the fabrication of the film takes place in a thin region (thickness on the order of e) called the dynamic meniscus, which joins the static meniscus to the film (Fig. 1). In the dynamic meniscus, the interface (of profile $h(x)$) is slightly curved and the flow nearly vertical. So the lubrication approximation can be used and the Navier-Stokes equation reduces to

$$\eta u_{yy} = p_x + \rho g = -\gamma h_{xxx} + \rho g, \qquad [1]$$

where $u(y)$ is the velocity profile inside the dynamic meniscus, p the Laplace pressure, and g the acceleration of gravity. The subscripts mean partial derivation.

As seen in Eq. [1], two different physical processes make the liquid flow in the dynamic meniscus: gravity (the plate is vertical) and capillary suction (the dynamic meniscus is curved). Equation [1] can be integrated using two boundary conditions: (i) no slippage at the wall: $u(y = 0) = V$; (ii) free liquid–air interface: $u_y(y = h) = 0$. Hence a parabolic profile for the velocity is obtained:

$$u(y) = \frac{1}{\eta}(-\gamma h_{xxx} + \rho g)\left(\frac{y^2}{2} - yh\right) + V. \qquad [2]$$

The flux of liquid per unit width of the plate is

$$Q = \int_0^h u dy = hV + \frac{h^3}{3\eta}(\gamma h_{xxx} - \rho g). \qquad [3]$$

In the steady-state regime, Q is a constant determined by matching the dynamic meniscus with the flat film ($h = e$, $h' = h'' = 0$; $u = V$):

$$Q = eV - \rho g e^3/3\eta. \qquad [4]$$

Introducing the latter expression in Eq. [3] and then Eq. [2] yields the surface velocity. In particular, it is easy to show that a stagnation point exists at the surface, at a thickness h^* given by

$$h^* = \left(3 - \frac{e^2\kappa^2}{\mathrm{Ca}}\right)e, \qquad [5]$$

where $\kappa^{-1} = \sqrt{\gamma/\rho g}$ is the capillary length and Ca the capillary number ($\mathrm{Ca} = \eta V/\gamma$).

The next step of the calculation consists of matching the dynamic meniscus with the static one, by expressing that there is no pressure difference between them at the point where they match. But the location of this point is unknown, so Landau, Levich, and Derjaguin performed an asymptotic matching, requiring the equality of the second derivatives of the profiles:

$$\left(\frac{d^2h}{dx^2}\right)^{\mathrm{dyn.}}_{h\to\infty} = \left(\frac{d^2h}{dx^2}\right)^{\mathrm{static}}_{h\to 0}. \qquad [6]$$

The static limit is the curvature at the top of the (static) meniscus, whose value is $\sqrt{2}\kappa$. To calculate the other limit, the curvature of the dynamic meniscus must be studied at large thicknesses. Dimensionless coordinates are introduced:

[1] To whom correspondence should be addressed.

$$h = eY$$
$$x = e\ \mathrm{Ca}^{-1/3} X. \qquad [7]$$

Taking Eq. [4] into account, Eq. [3] becomes:

$$Y''' = 3\,\frac{1 - Y}{Y^3} + \frac{e^2\kappa^2}{\mathrm{Ca}}\,\frac{Y^3 - 1}{Y^3}\,. \qquad [8]$$

To determine the first limit in Eq. [6], the latter equation must be integrated once. The integration is difficult to achieve with all the terms; we are looking for a constant limit for Y'', and Y''' obviously does not tend to zero as Y goes to infinity in Eq. [8] because of the gravity term.

It is first noted that two asymptotic solutions can be found according to the dominant mechanism causing the drainage in the dynamic meniscus, capillary suction or gravity, respectively expressed by the third derivative and the κ^2 term in Eq. [8].

2. THE VISCO-CAPILLARY REGIME

The LLD solution. If drainage by gravity can be neglected, Eq. [8] reduces to a differential equation free of any parameter,

$$Y''' = 3\,\frac{1 - Y}{Y^3}\,, \qquad [9]$$

with the conditions $Y \to 1$, $Y' \to 0$, and $Y'' \to 0$ for $X \to \infty$.

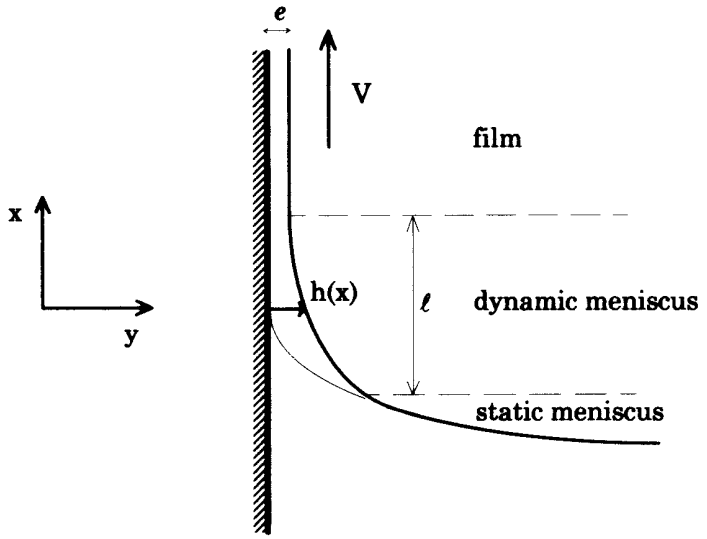

FIG. 1. Withdrawal of a plate out of a quiescent wetting liquid bath. The static meniscus is strained on a length l and a film of thickness e is entrained.

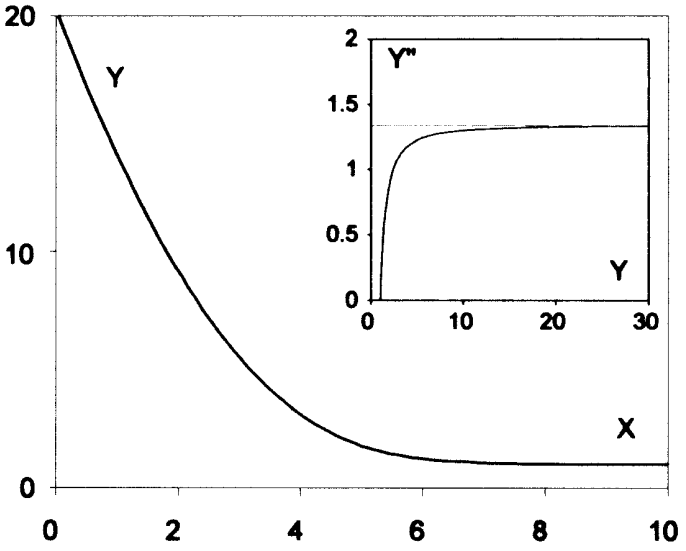

FIG. 2. Profile of the dynamic meniscus in dimensionless coordinates defined in [7], obtained by numerical integration of [9]. Insert: curvature Y″ vs Y, obtained by integration of [9].

Equation [9] can be integrated numerically once. The result is drawn in Fig. 2 and the sought-after limit is found:

$$\left(\frac{d^2Y}{dX^2}\right)^{\mathrm{dyn.}}_{Y\to\infty} = 1.34, \qquad [10]$$

which can be written, reintroducing h and x (see Eq. [7]), as

$$\left(\frac{d^2h}{dx^2}\right)^{\mathrm{dyn.}}_{h\to\infty} = 1.34\,\frac{\mathrm{Ca}^{2/3}}{e}\,. \qquad [11]$$

The static limit in Eq. [6] being $\sqrt{2}\kappa$, the Landau–Levich–Derjaguin (or LLD) law is finally obtained:

$$e = 0.94\ \kappa^{-1}\ \mathrm{Ca}^{2/3}. \qquad [12]$$

Domain of validity. Gravity was neglected in Eq. [8]. If e is given by Eq. [12], the approximation is justified if we have:

$$\mathrm{Ca}^{1/3} \ll 1. \qquad [13]$$

Hence, Eq. [12] is practically valid for very small capillary numbers ($\mathrm{Ca} < 10^{-3}$). Conversely, $\mathrm{Ca} = 1$ is expected to be the threshold above which drainage in the dynamic meniscus is mainly due to gravity.

Length of the dynamic meniscus. Close to the flat film, Eq. [8] can be linearized. Setting $Y = 1 + \epsilon$ (with $\epsilon \ll 1$) leads to

$$\epsilon''' = -3\epsilon\left(1 - \frac{e^2\kappa^2}{\mathrm{Ca}}\right). \qquad [14]$$

Making $\kappa^2 = 0$ yields a linear equation of solution: $\epsilon = e^{\sigma X}$, with $\sigma = -3^{1/3}$ (about -1.44). With the natural variables, the profile of the dynamic meniscus can be written

$$h(x) = e\left(1 + \exp\left(-\frac{x}{l}\right)\right), \quad \text{with} \qquad [15]$$

$$l \approx 0.69\, e\, \mathrm{Ca}^{-1/3}. \qquad [16]$$

l is the characteristic length of the dynamic meniscus pictured in Fig. 1. For very low capillary numbers (Eq. [13]), we have $e \ll l \ll \kappa^{-1}$; the extension of the dynamic meniscus is small compared with the size of the static meniscus but much larger than the film thickness, which justifies the lubrication approximation. Conversely, as Ca approaches unity, e and l both become on the order of the capillary length.

3. THE VISCO-GRAVITATIONAL REGIME

A convenient way to derive the asymptotic entrainment law in the gravity regime involves considering Eq. [14]. Without the capillary term ($\epsilon''' = 0$), we immediately find

$$e = \kappa^{-1}\sqrt{\mathrm{Ca}}. \qquad [17]$$

This asymptotic regime was first predicted by Derjaguin (3) using dimensional arguments: when the withdrawal velocity is important, capillarity becomes negligible and the thickness should no longer depend on the surface tension. Looking for a power law $e = \kappa^{-1}\mathrm{Ca}^n$ independent of γ gives $n = \frac{1}{2}$, as found in [17].

We can then be interested in the way the film gets thinner because of gravity after it is drawn. The thinning law of a vertical film of initial thickness e was first derived by Jeffreys (4). If the wall is immobile and the x-axis directed downward, the flux (per unit width of the plate) is given by Eq. [3]:

$$Q = \frac{\rho g h^3}{3\eta}, \qquad [18]$$

where h is now the film thickness depending on time and position x. The film dries upstream, so it gets thinner from the top. Conservation of matter yields:

$$\frac{\partial h}{\partial t} = -\frac{\partial Q}{\partial x} = -\frac{\rho g}{\eta} h^2 \frac{\partial h}{\partial x}. \qquad [19]$$

Equation [19] has two kinds of solutions: (i) a solution of constant thickness $h = e$, which is valid far below the top of the film (in this region, the flux of liquid is a constant given by Eq. [18]) and (ii) at the top of the film, Jeffreys has sought a power law solution for Eq. [19] ($h(x, t) = Ax^\alpha t^\beta$). If the origin of the x-axis is fixed at the top of the film, it is found that the profile is:

$$h(x, t) = \sqrt{\frac{\eta x}{\rho g t}}. \qquad [20]$$

This kind of slow thinning ($h \sim t^{-1/2}$) is known as a Reynolds-type law.

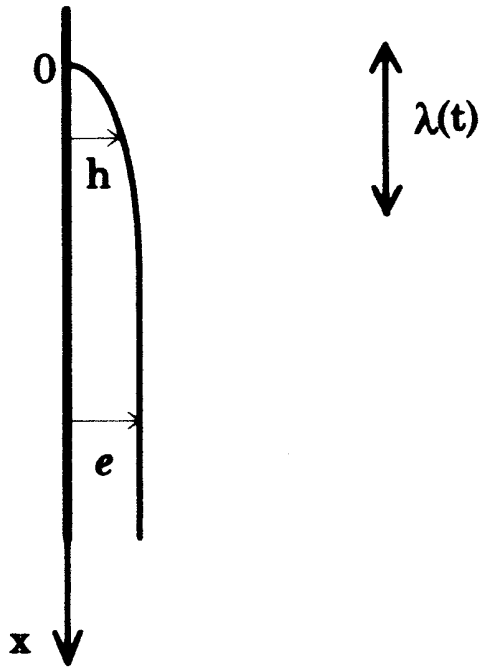

FIG. 3. Profile of a liquid film on a solid drained by gravity. e is the initial thickness of the film and λ the region close to the top where the film is thinned.

Figure 3 summarizes these results. As time goes on, a parabolic profile grows at the top of the film and matches the lower part, which remains at the initial thickness. The extension λ of the thinned zone is determined by matching the solution of Eq. [20] with $h = e$. It is thus found that λ increases linearly with time:

$$\lambda = \frac{\rho g}{\eta} e^2 t. \qquad [21]$$

Returning to the coating problem, we finally conclude that two types of withdrawal can be described, as sketched in Fig. 4. If $e < \kappa^{-1}\sqrt{\mathrm{Ca}}$, the thinned zone progresses more slowly than the film is made ($d\lambda/dt < V$), so that the film is flat everywhere but at the top (Fig. 4a). This case corresponds to the regime of entrainment limited by capillarity (see Section 2). If $e = \kappa^{-1}\sqrt{\mathrm{Ca}}$, the thinned zone progresses *at the same velocity as the plate*. The entrained

film is thinned everywhere, with a parabolic profile (Fig. 4b), and the Derjaguin equation (Eq. [17]) is only valid at the place where the film arises. The gravitational regime appears again as a borderline case; the film thickness cannot be larger than $\kappa^{-1}\sqrt{\mathrm{Ca}}$.

4. THE CROSSOVER BETWEEN THE TWO REGIMES

According to the mechanism causing the drainage in the dynamic meniscus, two asymptotic laws of liquid entrainment by a moving vertical plate have been found. At low capillary number ($\mathrm{Ca} < 10^{-3}$), the entrainment is limited by capillarity and described by Eq. [12]. At high capillary number, gravity is the principal cause of drainage and the entrainment law given by Eq. [17]. The latter regime is valid when $Ca^{1/3}$ is much larger than unity (see condition in Eq. [13]), and thus for $Ca > 10^3$. The crossover between the two regimes is especially broad since it concerns six orders of magnitude in capillary number. Therefore, it is worth studying the whole Eq. [8] with both the capillary and gravitational terms.

A first approach was performed by White and Tallmadge (5). Using Eq. [14], the linearized form of Eq. [8], they looked for an equivalent profile solution of the Landau problem. By this ingenious method, they finally obtained as a thickness dependence on the capillary number the simplest interpolation between the capillary and gravitational regimes:

$$\mathrm{Ca} = 1.09\, e^{3/2}\kappa^{3/2} + e^2\kappa^2. \qquad [22]$$

Here we propose a numerical solution of Eq. [8] and compare it with Eq. [22]. Following White and Tallmadge, the dimensionless quantity $T = e\kappa/\sqrt{\mathrm{Ca}}$ is introduced and treated as a parameter. Then Eq. [8] becomes

$$Y''' = \frac{1 - Y}{Y^3}\{3 - T^2(Y^2 + Y + 1)\}. \qquad [23]$$

According to the value of T, we discuss the possibility for Eq. [23] to have a solution which matches the flat film, when $X \to +\infty$, $Y \to 1$, $Y' \to 0$, and $Y'' \to 0$. For $T > 1$, there is no solution becoming flat at infinity. For $T = 1$, it can easily be seen in Eq. [23] that Y cannot be larger than unity. Thus, the law $e = \kappa^{-1}\sqrt{\mathrm{Ca}}$ is found again as an asymptotic regime.

For $0 < T < 1$, the profile $Y(X)$ can be deduced from the numerical integration of Eq. [23]. The procedure consists of starting from a point close to the flat film, whose coordinates are calculated from the linearized Eq. [14]. Then, the profile is integrated step by step using a Runge-Kutta method. Such a profile is pictured in Fig. 5. It is very different from the Landau case (Fig. 2b). A bump appears at small X, which is clearly unphysical in our problem. In other cases where the film has not to match a reservoir, but is bounded by a

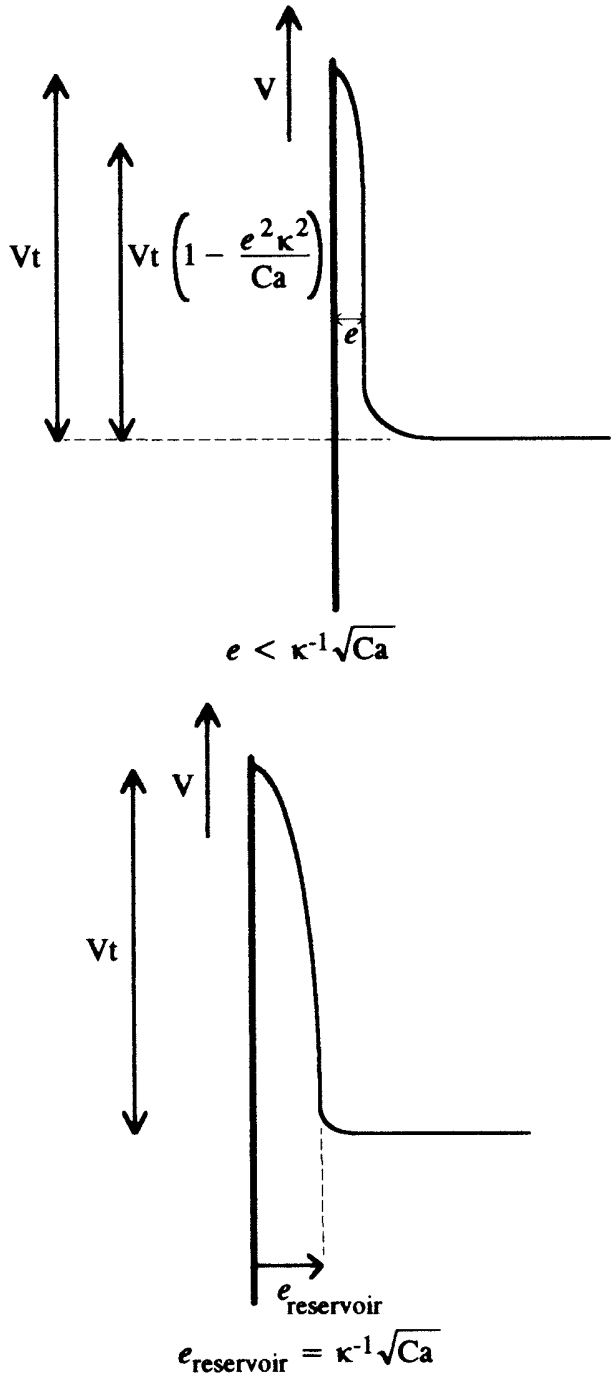

FIG. 4. Coating of a plate vertically withdrawn out of a reservoir. a) Visco-capillary regime, which corresponds to the LLD law [12]; the film is flat everywhere but at the top, where it is thinned. b) Visco-gravitational case, in which the film thickness is given locally by the Deryaguin law [17]; above this point, the whole film is thinned and has the parabolic profile given by [20].

contact line, rims indeed develop at the liquid front (and often break into vertical rivulets); that is the case for a film (bounded at its bottom by a contact line) flowing down a vertical plate (6).

When going from large X (the film) to small X (the reservoir) in Fig. 5, the second derivative of the profile passes through a maximum Y''_{M} before changing its sign at the

inflection point I. We propose matching the two menisci at this point. Such a matching allows us again to find the Landau solution at the limit $T \to 0$ (corresponding to $Ca \to 0$ or to the absence of gravity). At this limit, Y''_M tends towards 1.34 and Eq. [12] is recovered. This choice for the matching possibly overestimates the film thickness, since the maximum value of Y'' yields a maximum value for e.

Equation [6] is then used to determine the film thickness e. (Of course, this point is questionable; as Ca tends towards unity, the dynamic meniscus sweeps into the static one and finally makes it disappear.) Thus we write, as in the Landau case:

$$e = \frac{Y''_M}{\sqrt{2}} \kappa^{-1} \mathrm{Ca}^{2/3}. \qquad [24]$$

The resulting $T(\mathrm{Ca})$ dependence is drawn in Fig. 6, where it is compared with Eqs. [12], [17], and [22], and with the experimental data of Gutfinger and Tallmadge (7) and Spiers *et al.* (8). Though the numerical calculation possibly overestimates the film thickness, the results are found to be below the others.

A limitation of the calculation is that the expression of the curvature we used is only valid when the slope of the interface is small. This condition is not satisfied at the matching point. We introduce the exact curvature expression

$$C = -\frac{h''}{(1 + h'^2)^{3/2}}. \qquad [25]$$

Then, Eq. [23] becomes

$$Y''' = \frac{1 - Y}{Y^3}(3 - T^2(Y^2 + Y + 1)) \times (1 + Ca^{2/3}Y'^2)^{3/2} + \frac{3\mathrm{Ca}^{2/3}Y'Y''^2}{1 + \mathrm{Ca}^{2/3}Y'^2}. \qquad [26]$$

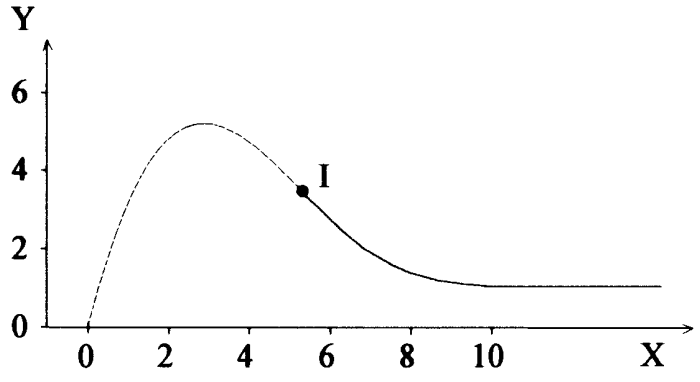

FIG. 5. Profile of the dynamic meniscus obtained by a numerical integration of Eq. [23] for $T = 0.71$. The main variation from Fig. 2 is the fact that the profile is not monotonous any longer, but presents a bump. The region beyond the inflection point I (dotted line) is unphysical in our problem.

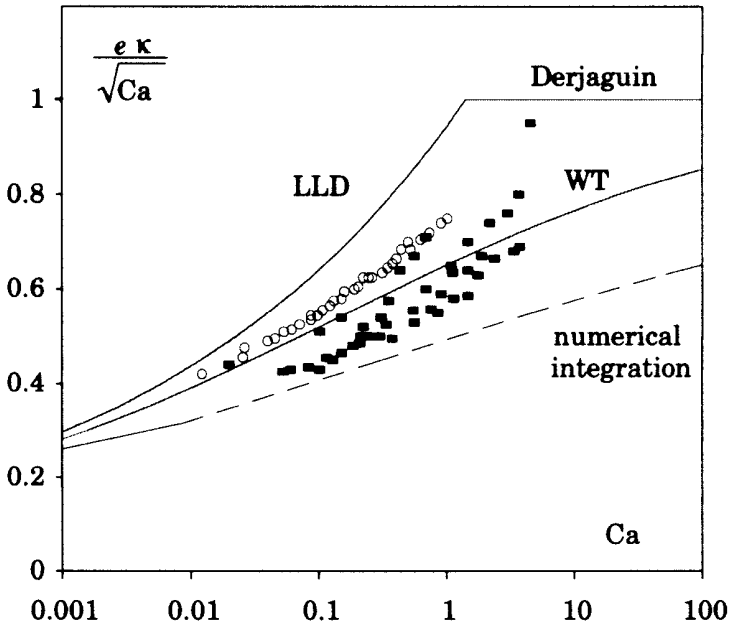

FIG. 6. Film thickness scaled by the Derjaguin thickness ($T = e\kappa/\sqrt{\mathrm{Ca}}$) as a function of the capillary number. In the same figure are presented the LLD law [12], the Derjaguin law [17], the White and Tallmadge cross-over [22], and the numerical integration of [23]. The squares are the experimental results of Gutfinger *et al.* (7) and the circles those of Spiers *et al.* (8), both obtained with glycerol–water solutions.

For a given value of Ca, the above equation can be numerically integrated following the same procedure as above. Then, the *maximum* T (for Y as large as possible) is sought by matching with the equation of the static meniscus, which can be written

$$Y'' - \sqrt{2}T\, Ca^{-1/6}((1 + \mathrm{Ca}^{2/3}Y'^2)^{1/2} + Ca^{1/3}Y')^{1/2} \times (1 + \mathrm{Ca}^{2/3}Y'^2)^{5/4} = 0. \qquad [27]$$

Results are drawn in Fig. 7. In Fig. 7a, an example of a profile is displayed. It can be seen that the matching with a reservoir is more realistic. In Fig. 7b, these numerical results are shown to fit in a satisfactory way the data of Spiers *et al.* (8) at low capillary numbers ($0.01 < \mathrm{Ca} < 0.2$). Then, when approaching $Ca = 1$, some discrepancies can be observed. We now discuss the main causes of these discrepancies.

5. THE VISCO-INERTIAL REGIME

Inertial effects may become nonnegligible at high withdrawal velocity. A Reynolds number associated with the flow inside the dynamic meniscus can be defined by taking as a characteristic length the thickness of the film ($Re = \rho V e/\eta$). Considering that the thickness is given by the LLD law (Eq. [12]), the Reynolds number can be written

$$Re \approx F\mathrm{Ca}^{5/3}, \quad \text{with} \quad F = \frac{1}{\eta^2}\sqrt{\frac{\rho\gamma^3}{g}}. \qquad [28]$$

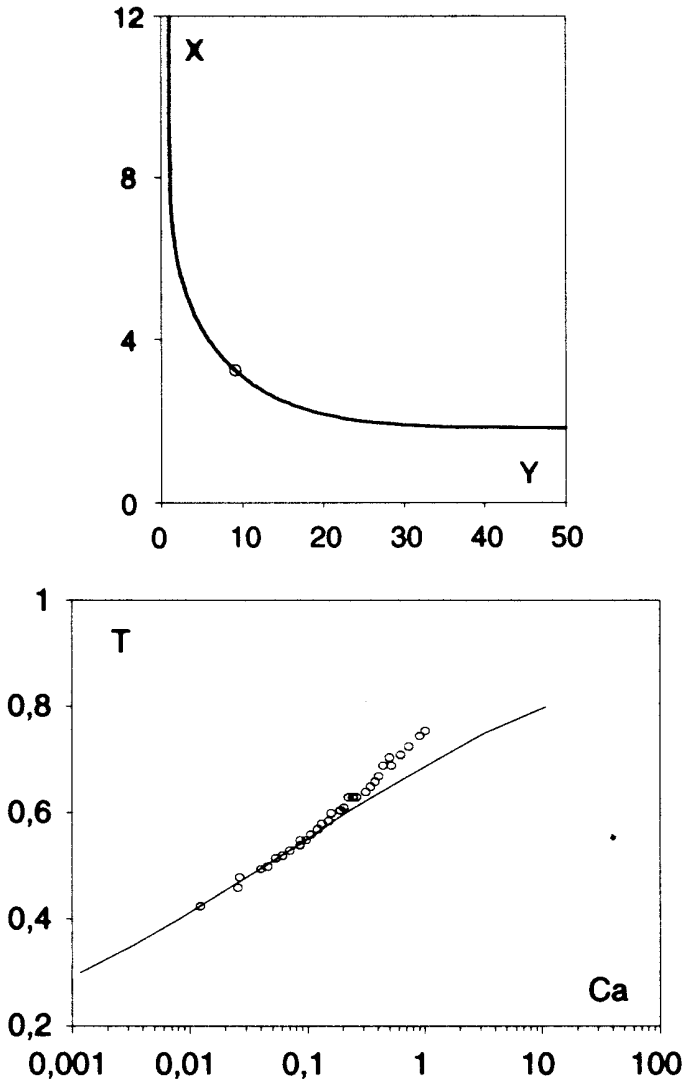

FIG. 7. (a) Profile of the dynamic meniscus obtained from an integration of [26] with $T = 0.5$ and $Ca = 0.044$. The circle gives the location of the matching point (Equation [27] is verified). (b) For the same coordinates as above (T versus Ca), numerical results from [26] are compared with the data of Spiers *et al.* (8).

The prefactor F depends only on the nature of the fluid, and varies mainly with the liquid viscosity. For a very viscous silicone oil ($\eta = 100\ P$), F is equal to 3×10^{-4}, and Re becomes larger than 1 if Ca is larger than 130 (which corresponds to $V \geq 25$ cm/s). For water, F is much larger ($F = 2 \times 10^5$), and a Reynolds number of order one is obtained for a very small capillary number ($Ca = 7 \times 10^{-4}$, which corresponds to $V = 5$ cm/s).

Thus, for liquids of low viscosity, inertia must be considered even at a very low capillary number (which justifies in this case taking Eq. [12] to define Re in Eq. [29]). We focus on this situation of practical importance (since water, with or without surfactants, is often used as a lubricant), which was not considered by previous authors. Soroka and Tallmadge (9) and Esmail and Hummel (10) studied the effect of inertia in plate coating for viscous liquids, for which, as seen above, both Reynolds and capillary numbers are large.

(a) Inertial Effects at Low Capillary Number

The inertial term of the Navier-Stokes equation must be incorporated in the Landau theory, which leads to a modified equation for the profile. The principle of the calculation was first proposed by Esmail and Hummel (10) and developed recently by de Ryck (11) and Koulago (12): it consists of supposing that the flow inside the meniscus still has a parabolic profile, but that the effective pressure which provokes it is unknown. Writing the Navier-Stokes equation (with the usual boundary conditions) allows a more general expression for the profile of the dynamic meniscus to be found. Written with the dimensionless variables of Landau, it reads:

$$\left[\frac{Y''}{(1 + \mathrm{Ca}^{2/3} Y'^2)^{3/2}}\right]' = \frac{1 - Y}{Y^3}\{3 - T^2(Y^2 + Y + 1)\} + \frac{1}{5} F \mathrm{Ca}^{11/6} T\left(Y^2 - \frac{2}{3}(3 - T^2)^2\right)\frac{Y'}{Y^3}. \quad [29]$$

The first part of the equation is Eq. [23], written with the whole expression for the curvature, given by Eq. [25]. The second term in the right member is the inertial contribution, which logically includes the number F. This term is not negligible in the case in which we are interested, since F was shown to be large for liquids of low viscosity.

Equation [29] can be integrated as explained above, which allows us to determine the maximum of the curvature. Then matching provides the film thickness, which can be expressed as a function of the capillary number. The results are displayed in Fig. 8 for $F = 2 \times 10^5$ (water) and $F = 10^4$ (long alkane).

A remarkable feature can be observed in Fig. 8: *inertia provokes a thickening of the film above a threshold in capillary number*. The threshold Ca* depends on the nature of the liquid: the higher F, the smaller Ca*. A simple way to understand this effect physically is the following: the plate puts the liquid close to it in motion, and the effect of inertia is indeed to project the liquid at the exit of the dynamic meniscus out of the reservoir, and thus to thicken the film. This argument helps to understand the limitation of this effect: at still higher velocities, the problem may become unstationary. The plate does not spend enough time in the bath to put a thick layer of liquid in motion, so the film is limited to the viscous boundary layer which develops in the bath. In this case, the thickness decreases with the velocity.

Such effects were recently reported in fiber withdrawal experiments (13). The thickening effect was observed and found to be more spectacular than in Fig. 8 since gravity (a natural factor for limiting the thickness) could be neglected (experiments were performed at small Bond numbers). Be-

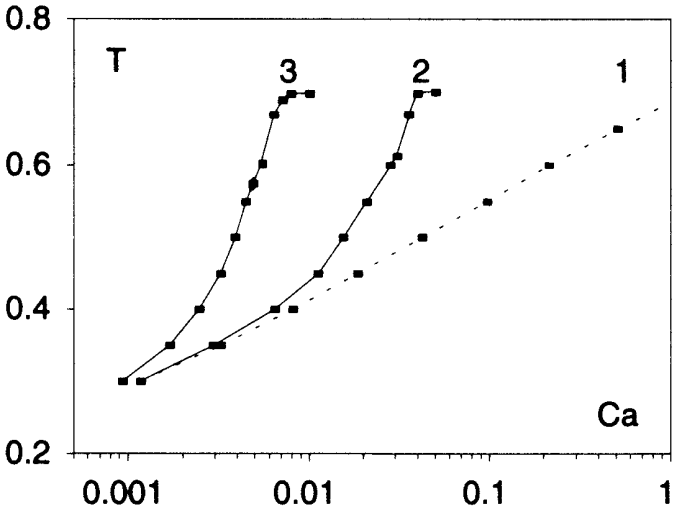

FIG. 8. Effect of inertia on the film thickness, obtained by integrating Eq. [29] numerically. $T = e\kappa/\sqrt{\mathrm{Ca}}$ is plotted vs the capillary number Ca for three different values of the number F (defined in Eq. [28]): (1) $F = 0$ (liquid of large viscosity); (2) $F = 10^4$ (corresponding to a long alkane); and (3) $F = 2 \times 10^5$ (corresponding to pure water). When F is large, the effect of inertia is to increase the film thickness above a threshold in capillary number.

sides, a scaling argument was proposed (and checked experimentally), for predicting the location of the threshold: inertia provokes a large thickening when the dynamic pressure (of order ρV^2) is equal to the Laplace pressure (of order γ/r, with r being the fiber radius). For a plate, we expect inertia to be important in a similar way when ρV^2 becomes of the same order as $\rho g \kappa^{-1}$, the hydrostatic pressure in the meniscus, which gives as a threshold:

$$\mathrm{Ca}^* \approx \frac{1}{\sqrt{F}} . \qquad [30]$$

Another way to derive this threshold consists of considering the inertial term in Eq. [29], which must be considered when the quantity $F\mathrm{Ca}^{11/6}T$ is of order one. Since we are at low capillary number, the thickness (in the expression of T) is given by the LLD law ($e \approx \mathrm{Ca}^{2/3}$), which finally yields Eq. [30]. For water, we find $\mathrm{Ca}^* = 2 \times 10^{-3}$ (or $V \approx 16$ cm/s), in good agreement with the threshold observed in curve 3 of Fig. 8. For $F = 10^4$, the difference from the curve without inertia appears at around $\mathrm{Ca}^* = 0.01$, as predicted by Eq. [30]. Ca^* may be written as

$$V^* \approx \sqrt{\kappa^{-1} g}, \qquad [31]$$

showing that inertia becomes important when the withdrawal velocity is close to the minimal velocity of capillaro-gravitational waves (typically 10–30 cm/s).

To the best of our knowledge, there is only one experiment corresponding with these features (large Reynolds numbers and small capillary numbers), which is due to Tallmadge and Stella (14). Data on the coating of a plate with water are reported, and indeed a sharp increase of the film thickness above the LLD law is observed. A remarkable point (stressed by the authors) is the fact that the discrepancy is found at very low capillary numbers (thicknesses were reported for $10^{-4} < \mathrm{Ca} < 10^{-3}$), in agreement with our description. Of course, new data would be useful to test our predictions quantitatively.

Note finally that the diverging behavior in Fig. 8 exhibits some inflection (and saturation). The last point for each curve may have no real significance; it corresponds to conditions for which the numerical integration of Eq. [29] becomes hard to achieve, since solutions have oscillations which make matching difficult. That is why our results stop at that point; it was impossible to produce a meaningful solution for any further increase in capillary number.

(b) When Ca ≥ 1

We do not describe the case where both Reynolds and capillary numbers are larger than unity. Spiers *et al.* (8) who have made attempts to describe this case, have shown that the incorporation of the strain-rate component in the equilibrium condition of the liquid–air interface leads to a slight thickening of the film. On the other hand, Esmail and Hummel (10) incorporated the same term in their inertial theory of free coating. Their results, performed for F ranging between 0 and 77, do not show a diverging behavior.

6. SUMMARY AND CONCLUDING REMARKS

We proposed a numerical solution of the gravity-corrected Landau theory for plate coating, based on a new matching and on the consideration of the exact expression of the curvature in order to obtain realistic profiles. Then, we discussed an improvement of practical importance: if the withdrawal velocity becomes higher than a threshold, inertia must be taken into account. We discussed the particular case of liquids of low viscosity (aqueous solutions), for which the capillary number can remain much smaller than unity even if the Reynolds number becomes of order one (or larger). In that case, a thickening of the film is predicted because of the influence of inertia, which ejects the fluid out of the reservoir. The observations of Tallmadge and Stella could be related to this effect, but new specific experiments would be useful to test it.

The case where both the velocity and the capillary numbers are large is the most complicated and remains to be fully solved. In this case, the lubrication approximation is no longer justified (a two-dimensional flow must be taken into account) and the matching with a static meniscus becomes questionable.

ACKNOWLEDGMENTS

It is a pleasure to thank V. Shkadov and M. Velarde for very useful discussions.

REFERENCES

1. Landau, L., and Levich, B., *Acta Physicochim. USSR* **17,** 42 (1942).
2. Derjaguin, B., *Acta Physicochim. USSR* **20,** 349 (1943).
3. Levich, V. G., ''Physical Hydrodynamics.'' Prentice-Hall, Englewood Cliffs, NJ, 1962.
4. Jeffreys, H., *Proc. Cambridge Philos. Soc.* **26,** 204 (1930).
5. White, D. A., and Tallmadge, J. A., *Chem. Eng. Sci.* **20,** 33 (1965).
6. Huppert, H. E., *Nature* **300,** 427 (1982).
7. Gutfinger, C., and Tallmadge, J. A., *AIChE J.* **11,** 403 (1965).
8. Spiers, R. P., Subbaraman, C. V., and Wilkinson, W. L., *Chem. Eng. Sci.* **29,** 389 (1974).
9. Soroka, A. J., and Tallmadge, J. A., *AIChE J.* **17,** 505 (1971).
10. Esmail, M. N., and Hummel, R. L., *AIChE J.* **21,** 958 (1975).
11. De Ryck, A., and Quéré D., *C. R. Acad. Sci. Sér. II Paris* **317,** 891 (1993).
12. Koulago, A., Quéré, D., de Ryck, A., and Shkadov, V., *Phys. Fluids* **7,** 1221 (1995).
13. De Ryck, A., and Quéré, D., *J. Fluid Mech.* **311,** 219 (1996).
14. Tallmadge, J. A., and Stella, R., *AIChE J.* **14,** 838 (1968).